Fermions at Finite Density in the Nonrelativistic Gauge/Gravity Duality

by

Raghu Mahajan

Submitted to the Department of Physics
in partial fulfillment of the requirements for the degree of

Bachelor of Science in Physics

at the

MASSACHUSETTS INSTITUTE OF TECHNOLOGY

February 2011

Author .....

Department of Physics
December 22, 2010

Certified by.

Allan W. Adams
Assistant Professor
Thesis Supervisor

Accepted by .....

Nergis Mavalvala
Senior Thesis Coordinator, Department of Physics

Fermions at Finite Density in the Nonrelativistic Gauge/Gravity Duality

by

Raghu Mahajan

Submitted to the Department of Physics
on December 22, 2010, in partial fulfillment of the
requirements for the degree of
Bachelor of Science in Physics

Abstract

The AdS/CFT correspondence has provided a new tool to investigate strongly correlated systems in condensed matter physics. This thesis presents the computation of retarded fermion Green functions at finite density and zero temperature in the nonrelativistic gauge/gravity duality. We find evidence of Fermi surfaces and investigate their properties. We show that the near-horizon scaling dimension, an important quantity that controls the low-energy excitations of the theory, depends on the momentum along the "extra" direction in nonrelativistic gauge/gravity duality.

Thesis Supervisor: Allan W. Adams
Title: Assistant Professor

Acknowledgments

I would like to thank my supervisor, Professor Allan Adams for all the guidance and encouragement during this project, especially during the initial learning phase when all the material for this thesis was new to me. I would also like to thank Juven Wang and Professor John McGreevy for numerous insightful discussions. I am indebted to my parents who have supported me in all my decisions, and without whose toil and sacrifices it would have been impossible for me to study at MIT. My thanks are also due to Professor Vijay Singh and Arvind Chauhan, my physics teachers and mentors who nurtured and encouraged my love of physics in my high school days.

Contents

Chapter 1

Overview

1.1 Previous Literature

The AdS/CFT correspondence, or the gauge/gravity duality was originally proposed in 1997 by Maldacena [1] and further developed in [2] and [3]. According to this proposition, a theory of gravity in $(n+1)$-dimensional asymptotically AdS space is dual to a field theory living on the n-dimensional boundary of the asymptotically AdS space.

The duality has important implications for high-energy theory, including a possible resolution of the blackhole information paradox [4], [5]. The resolution of this paradox was indeed one of the motivations that led to the discovery of AdS/CFT correspondence. Further, the AdS/CFT correspondence is a concrete realization of the holographic principle [6] and provides a non-perturbative definition of quantum gravity in AdS space in terms of the dual field theory. Reference [7] provides a comprehensive review of AdS/CFT from a string theory standpoint.

Gauge/gravity systems have also inspired optimism on a different front: strongly interacting condensed matter systems. Holography allows us to translate questions in strongly-coupled field theories to dual problems in weakly-coupled gravity, providing new approaches to classic problems. Due to this, a more hands-on approach to studying gauge/gravity systems has been advertised; the articles [8], [9], [10], and [11] are tutorial introductions to such a phenomenology-inspired approach to holographic

duality.

As a simple example, the physics of a charged scalar field in the spacetime of an AdS Reissner-Nordstrom blackhole reproduces the physics of a superconductor [12], [13], [14]. The study of the fermion field in the same background yields gapless excitations around Fermi surfaces with quasiparticle like poles in the spectral function of the boundary operator; see [15], [16]. In [16], marginal Fermi surfaces were found which correspond to the strange metal phase of high-T_c superconductors. Building on this correspondence, it was shown in [17, 18] that the contribution of the Fermi surface to the resistivity has linear temperature dependence, a signature of the strange metal phase. Very recently there has been a concrete proposal by Sachdev [19] that the behavior of fermions in these systems closely corresponds to the fractionalized Fermi liquid phase of the lattice Anderson model, which is a candidate theory for explaining the behavior of strange metals. This is important since it identifies a precise theory applicable to an experimentally-realizable system for which the correspondence might be valid. For more on fractionalization and relation of holography to strange metals, see [20],[21], [22]. Further, coupling the fermion field to a condensed massless scalar field using a Majorana-mass type term in an extremal background gives rise to a gapped spectrum; see [23].

Dual descriptions have also been found for the quantum Hall effect [24], the Nernst effect [25, 26, 27] and the de Haas-van Alphen effect [28].

One of the cornerstones of the AdS/CFT correspondence is that the group of isometries of AdS_{n+1} is isomorphic to the conformal group in n spacetime dimensions. The conformal group is an extension of the Poincare group, the symmetry group of the free Klein-Gordon equation.

It is thus natural to ask if there are spacetimes whose isometries realize the conformal extension of the symmetry group of the nonrelativistic Schrödinger equation. Such a metric was first found in [29] and [30]. However this system has the peculiar property that the dimension of the spacetime geometry is *two* more than the "boundary" field theory. Apart from the usual radial direction of AdS/CFT, there is a circle, the momentum along which is related to the invariant particle number

in nonrelativistic conformal field theories. Fermion Green functions for this vacuum Schrödinger metric were calculated in [31]. It has only recently been shown that one can preserve the correspondence after a Kaluza-Klein reduction of this compact dimension [32].

Solutions with finite temperature in the nonrelativistic case were constructed in [33], [34], [35]. These solutions did not have a clean extremal limit. This problem was addressed in [36] and [37] and solutions were constructed with proper extremal limits by adding extra fields, including a Maxwell field.

1.2 Goal of this Thesis

The goal of this thesis is to study Fermi surfaces in nonrelativistic CFTs at zero temperature and finite density. We do this by studying the retarded Green function for fermionic operators dual to bulk fermions in blackhole backgrounds constructed in [36] and [37]. The reasons for the studying this system are several-fold. First, many condensed matter systems that one studies in lab have nonrelativistic conformal invariance and it would be encouraging to see the robustness of Fermi surfaces in this setting. Second, the momentum along the extra circle in the geometry is expected to lead to effects that are not observed in the AdS case. Indeed, the AdS_2 scaling dimension, a critical quantity that controls the low-frequency behavior of the spectral functions, depends on this momentum. Third, the Dirac equation studied in [15], [16] is separable into two independent equations for the eigenvalues of the retarded Green function. This is not the case in charged Schrödinger blackhole geometry, and might lead to a gapped system, as in [23].

By looking at the spectral function, we find Fermi surfaces for a range of values of the parameters in our system. This shows the robustness of holographic Fermi surfaces in the nonrelativistic setting. We also calculate the near-horizon scaling exponent and show that it depends on the momentum along the "extra" dimension in the nonrelativistic setting. The Fermi surface does not exist for parameter values such that the IR scaling dimension is imaginary.

Chapter 2

Background

In this chapter we give some background on the foundational concepts that we will need. We give a quick introduction to anti deSitter spaces and conformal field theories. We explain in some detail the AdS/CFT correspondence. Finally, we introduce the retarded Green function and show how it is computed from the AdS/CFT correspondence.

2.1 Anti deSitter space $\mathbf{AdS}_{n+1}$

This section is largely based on the treatment of AdS spaces given in Barton Zwiebach's book on string theory [38].

We use the notation $\mathbb{R}(p,q)$ to denote the space $\mathbb{R}^{p+q}$ with the flat metric $\eta = \text{diag}(-,\cdots,-,+,\cdots,+)$ with p minuses and q plusses. We define $SO(p,q)$ to be the group of proper Lorentz transformations of $\mathbb{R}(p,q)$.

2.1.1 Hyperbolic Space: $\mathbb{H}_n$

Consider the surface in $\mathbb{R}(1,n)$ defined by the constraint

$$-(x^0)^2 + (x^1)^2 + \cdots + (x^n)^2 = -R^2, \tag{2.1}$$

where R is a positive real number. This surface consists of two disconnected sheets (one for $x^0 \geq R$ and one for $x^0 \leq -R$). The *Hyperbolic space* $\mathbb{H}_n$ is defined to be one of these sheets. For definiteness, let us pick the sheet with $x^0 \geq R$.

Our task is to construct a convenient coordinate chart on $\mathbb{H}_n$ and to write the induced metric in terms of these coordinates.

We define the coordinates $(\xi_1, \ldots, \xi_n)$ of a point P in $\mathbb{H}_n$ by stipulating that the point $(0, \xi_1, \ldots, \xi_n)$ lie on the line joining P to the point $(-R, 0, \ldots, 0)$. This is stereographic projection. A simple calculation reveals

$$\xi^i = \frac{R^2 - r^2}{2R^2} x^i, \tag{2.2}$$

where we have introduced $r = \sqrt{(\xi^1)^2 + \cdots + (\xi^n)^2}$.

The x^0-coordinate of the point on $\mathbb{H}^n$ is given by

$$x^0 = \frac{R^2 + r^2}{R^2 - r^2} R. \tag{2.3}$$

We now rescale the ξ^i's by sending ξ^i to $R\xi^i$, and substitute the above expressions into the metric on $\mathbb{R}(1, n)$ to get the $\mathbb{H}_n$ metric:

$$ds^2 = 4R^2 \frac{d\xi^i d\xi^i}{(1 - r^2)^2}, \tag{2.4}$$

where the index i runs from 1 to n and $r^2 = (\xi^1)^2 + \cdots (\xi^n)^2 < 1$.

Note that the conformal boundary of $\mathbb{H}_n$ is S^{n-1}, defined by $r = 1$.

2.1.2 AdS space: $\mathbf{AdS}_{n+1}$

Now consider the space $\mathbb{R}(2, n)$ with coordinates $(u, v, x^1, \ldots, x^n)$. The space AdS_{n+1} is defined to the surface in this space that obeys the following constraint:

$$-u^2 - v^2 + (x^1)^2 + \cdots + (x^n)^2 = -R^2. \tag{2.5}$$

Note that this differs from hyperbolic spaces in only that there is an extra timelike direction.

We define the coordinates z and t to be the radial and angle coordinates in the $u-v$ plane, that is, $u = z\cos t$ and $v = z\sin t$. The constraint now becomes $-z^2 + x^i x^i = -R^2$ which is exactly the constraint for hyperbolic spaces. Now we can use our ξ^i coordinates from the last section and write the AdS_{n+1} metric as

$$\begin{aligned} ds^2 &= -z^2 dt^2 + (-dz^2 + dx^i dx^i) && (2.6) \\ &= R^2\left[-\left(\frac{1+r^2}{1-r^2}\right)^2 dt^2 + \frac{4d\xi^i d\xi^i}{(1-r^2)^2}\right]. && (2.7) \end{aligned}$$

Note that the conformal boundary of AdS_{n+1} is $\mathbb{R}\times S^{n-1}$. Note also that because of form of the equation that embeds AdS_{n+1} in $\mathbb{R}(2,n)$, the group of isometries of AdS_{n+1} is $SO(2,n)$.

Next, we construct new coordinates on AdS_{n+1} in which we will actually be working. Isolate x^n out of the x^i's and define the new coordinates t, r and y^i for $i = 1,\ldots,n-1$ as follows:

$$v + x^n = \frac{r}{R}, \quad u = \frac{r}{R}t, \quad x^i = \frac{r}{R}y^i.$$

Solve for $x^n - v$ using Eq.(2.5) and a straightforward computation yields

$$ds^2 = \frac{r^2}{R^2}(-dt^2 + dy^i dy^i) + \frac{R^2}{r^2}dr^2. \tag{2.8}$$

In these coordinates, the conformal boundary is at $r = \infty$.

The AdS_{n+1} space is a solution to Einstein's equations derived from the Einstein-Hilbert action with a negative cosmological constant. Explicitly, the action is given by

$$S = \frac{1}{2\kappa^2}\int d^{n+1}x\sqrt{-g}\left[\mathcal{R} + \frac{n(n-1)}{R^2}\right], \tag{2.9}$$

where $\mathcal{R}$ is the Ricci scalar, κ is the gravitational constant and R is the curvature-radius of the AdS space.

2.1.3 Adding blackholes to AdS

We now add a Maxwell field to the above action to get the new action

$$S = \frac{1}{2\kappa^2}\int d^{n+1}x\sqrt{-g}\left[\mathcal{R} + \frac{n(n-1)}{R^2} - \frac{R^2}{g_F^2}F^2\right], \tag{2.10}$$

where g_F is the dimensionless gauge-coupling (the Maxwell potential A has length dimension -1).

A solution to the Einstein-Maxwell equations generated by the action in Eq.(2.10) is given by

$$ds^2 = \frac{r^2}{R^2}(-f dt^2 + d\vec{x}^2) + \frac{R^2}{r^2}\frac{dr^2}{f}, \tag{2.11}$$

which is obtained by multiplying the dt^2 term and dividing the dr^2 term in Eq.(2.8) by the function f, which we now describe. The function f contains two parameters: the black-hole charge Q, and the blackhole horizon radius r_0. In terms of these parameters,

$$f(r) = 1 + \frac{Q^2}{r^{2n-2}} - \left(r_0^n + \frac{Q^2}{r_0^{n-2}}\right)\frac{1}{r^n}. \tag{2.12}$$

Note that $f(r_0) = 0$. The temperature of the black-hole is proportional to $f'(r_0)$ and is given by

$$T = \frac{nr_0}{4\pi R^2}\left(1 - \frac{n-2}{n}\frac{Q^2}{r_0^{2n-2}}\right). \tag{2.13}$$

The other part of the solution, the Maxwell potential A_μ, has only one component A_t given by

$$A_t(r) = \mu\left(1 - \left(\frac{r_0}{r}\right)^{n-2}\right), \tag{2.14}$$

where μ is given by

$$\mu = \sqrt{\frac{n-1}{2(n-2)}}\frac{g_F Q}{R^2 r_0^{n-2}}. \tag{2.15}$$

Note that this means that the magnetic field is zero and the electric field is radial.

The geometry becomes extremal when $f(r)$ has a double root at r_0. In this case, the temperature is zero, and $Q = \sqrt{n/(n-2)}r_0^{n-1}$.

2.2 Basics of CFT

2.2.1 The Conformal Group

The conformal transformations of $\mathbb{R}(p,q)$ are defined to be the set of coordinate transformations that leave the metric unchanged up to a scale factor that can vary from point to point. That is, if $x^\mu \to x'^\mu$ is a conformal transformation, we require that

$$\frac{\partial x^\rho}{\partial x'^\mu}\frac{\partial x^\sigma}{\partial x'^\nu}\eta_{\rho\sigma} = \lambda(x)\eta_{\mu\nu}. \tag{2.16}$$

From this we can conclude that for $x^\mu \to x^\mu + \epsilon^\mu(x)$ to be a conformal transformation, we must have

$$\frac{\partial_\mu \epsilon_\nu + \partial_\nu \epsilon_\mu}{2} = \frac{\partial \cdot \epsilon}{p+q}\eta_{\mu\nu}. \tag{2.17}$$

Note that the usual Poincaré transformations are conformal transformations with the additional requirement that $\lambda(x) = 1$. Conformal transformations also include scale transformations and special conformal transformations, which are translations preceded and followed by inversions in the unit sphere (of appropriate dimensions).

It is possible to deduce that the conformal group of $\mathbb{R}(p,q)$ is isomorphic to $SO(p+1, q+1)$. In particular the conformal group of $\mathbb{R}(1, n-1)$ is isomorphic to $SO(2,n)$, which is the set of isometries of AdS_{n+1}.

2.2.2 Conformal field theory

A conformal field theory is a field theory whose action is invariant under the conformal group. A classic example is that of a massless scalar field in the Euclidean plane, $\mathbb{R}(0,2)$. The action is

$$S = \frac{1}{2}\int dxdy \left[\left(\frac{\partial\phi}{\partial x}\right)^2 + \left(\frac{\partial\phi}{\partial y}\right)^2\right]. \tag{2.18}$$

To see why the action is invariant under conformal transformations, note that the conditions in Eq.(2.17) reduce to the Cauchy-Riemann equations for ϵ^0 and ϵ^1. In-

troducing the complex coordinates $z = x + iy$ and $\bar{z} = x - iy$, we can restate the above result as stating that the conformal transformations are holomorphic functions $z' = f(z)$. Rewriting the action as

$$S = \int dz d\bar{z}\ \partial_z \phi\, \partial_{\bar{z}} \phi, \tag{2.19}$$

we can immediately see that it is invariant under conformal transformations.

However, in most CFTs, we do not start with a classical action and quantize it. It is possible to study CFTs by exploiting the symmetries, without knowing the explicit form of the action. For example, the two-point and three-point functions of "quasi-primary" fields (a quasi-primary field is a field that transforms by powers of $\partial f/\partial z$ and $\partial \bar{f}/\partial \bar{z}$) in any CFT on the Euclidean plane is determined by symmetries alone.

2.3 Introduction to AdS/CFT

The original paper by Juan Maldacena [1] posits an equivalence between two specific theories. One of them is type IIB string theory in the 10-dimensional space $AdS_5 \times S^5$, and the second is the maximally supersymmetric ($\mathcal{N} = 4$) $SU(N)$ gauge theory in $3 + 1$ dimensions in the 't Hooft limit.

We will not delve into the details of those theories; suffice it to say that they have inspired an "engineering" approach to AdS/CFT. A model is constructed and the legitimacy is conferred by the results and phenomena the model can produce. We collect below the main ideas that will be relevant for our study. For a more detailed tutorial introduction to this phenomenology-inspired approach, please refer to [8], [9], [10], [11].

The minimum ingredients for holographic models are an $(n + 1)$-dimensional asymptotically AdS space and a field theory on the boundary. Below, we will refer to the $(n + 1)$-dimensional space as the *bulk*. Operators in the boundary field theory correspond to fields in the bulk gravity theory.

1. A scalar field of mass m corresponds to a scalar operator with scaling dimension

$n/2 + \sqrt{m^2R^2 + n^2/4}$.

2. A fermion spin-1/2 field of mass m corresponds to a fermion spin-1/2 operator of scaling dimension $mR + n/2$. If n is odd, both the boundary and the bulk spinors are Dirac spinors. However, if n is even, then a Dirac spinor in the bulk corresponds to a chiral spinor in the boundary theory; see [39].

3. The metric tensor in the bulk is dual to the stress-tensor of the boundary theory.

4. If there is a conserved vector current J^μ associated with a $U(1)$ symmetry in the boundary theory (e.g. particle number), it is dual to a gauge field A^μ in the bulk. In the case of a conserved particle number the boundary value of the gauge field determined the chemical potential conjugate to the particle number. Thus, a finite number-density in the field theory corresponds to an AdS blackhole with charge. In general, global symmetries in the boundary theory correspond to local symmetries is the bulk.

Lets take the case of a scalar field ϕ in the bulk that corresponds to a scalar operator $\mathcal{O}$ in the boundary theory. The boundary value ϕ_0 of the field ϕ acts as a source for the scalar $\mathcal{O}$, giving a term

$$S_{\text{int}} = \int d^n x \, \phi_0 \mathcal{O} \tag{2.20}$$

in the action of the boundary theory.

The central result that we will use is that the partition function of the boundary field theory is given by the on-shell action of the bulk gravity theory [2] [3]:

$$\boxed{Z_{\text{CFT}}[J] = e^{-S_{\text{grav}}(\phi)|^{\phi_0=J}_{\text{on-shell}}}}. \tag{2.21}$$

Putting the system at a finite temperature T maps to introducing in the geometry a blackhole with Hawking temperature T. When the function $f(r)$ that appears in Eq.(2.11) has a double root at the horizon, the geometry is extremal, which corresponds to zero temperature.

It should be noted that it is possible to interpret the extra dimension in the bulk as being associated with the Renormalization Group (RG) flow in the boundary theory; see [40]. The horizon of the blackhole corresponds to the low-energy IR sector of the field theory and the boundary corresponds to the high-energy UV sector of the field theory.

2.4 Green Functions from AdS/CFT

The experimental study of a physical system usually involves measuring the response of a system of weak perturbations. Responses to weak perturbations are linear, that is, they are proportional to the perturbation. Examples of linear responses include elasticity, magnetic susceptibility, conductivity, and many others. Due to their importance in the characterization of a physical system, it is important for a theory to predict the linear responses of a system.

For a beginner's introduction to Green functions and their formal properties please see Appendix A.

Consider two operators A and B in a field theory in n spacetime dimensions. Suppose we apply a perturbation to the system, leading to a change in the Hamiltonian of the system by

$$\delta H(t) = \int d^{n-1}x \ \phi(t,x)B(x). \tag{2.22}$$

We wish to study the change in the expectation value of the operator A due to the perturbation δH. Since the perturbation is small, we expect that in frequency space

$$\delta\langle A\rangle(\omega,k) = G^R(\omega,k)\phi(\omega,k). \tag{2.23}$$

The quantity G^R is called the *retarded Green function.* It can be shown that Eq.(2.23) is satisfied by

$$G^R(\omega,k) = -i\int d^{n-1}xdt \ e^{i\omega t - ik\cdot x}\theta(t)\langle[A(t,x),B(0,0)]\rangle. \tag{2.24}$$

It can also be shown that the retarded Green function is analytic in the upper half of the complex ω plane. See, for example, [8] for a proof of these two properties.

We will be interested in the case when A is a fermionic spin-1/2 operator and B is its hermitian conjugate.

Consider the correspondence between the partition function of the boundary theory and the on-shell action of the bulk theory (Eq.(2.21)), and the structure of the boundary Lagrangian (Eq.(2.20)). By differentiating with respect to ϕ_0, we can conclude that the expectation value $\langle \mathcal{O} \rangle$ is given by the conjugate momentum Π of the bulk field, evaluated on-shell. This is because the derivative of the on-shell action with respect to a field is its conjugate momentum. This leads us to a simple recipe for the retarded Green function, due to Iqbal and Liu [41]:

$$G^R = \lim_{r \to \infty} \frac{\Pi}{\phi}. \tag{2.25}$$

However, there is one more detail, which we now discuss.

Let us look in more detail how we would compute the Green function. Consider a scalar field ϕ. Since the equation of motion for ϕ is second-order, we need two initial conditions to integrate. This means that we need to specify a boundary condition to uniquely specify the right hand side of Eq.(2.25).

By analyzing the behavior of the equation of motion near the boundary, we determine the leading behavior of the field ϕ as $r \to \infty$. The general AdS case yields $\phi \to A r^{\Delta_+} + B r^{\Delta_-}$ where Δ_+ and Δ_- are fixed in terms of the mass, charge and number of dimensions but A and B are arbitrary.

Assuming Δ_+ is bigger than Δ_-, we can impose Dirichlet boundary conditions on A. This is because the term with A is the leading term and is thus interpreted as the source term for the dual boundary operator. The quantity B is then the response.

Now, near the horizon, a general solution will be a superposition of an incoming wave and an outgoing wave. It is known that to compute the retarded Green function, we need to have a purely incoming wave. This provides us with another boundary condition. In the Euclidean signature, an incoming wave corresponds to a solution

that is regular.

Note that at the linear level, $G^R = B/A$ will be independent of the Dirichlet boundary condition on A, since B would be directly proportional to A. Thus, by imposing the infalling boundary condition at the horizon and integrating the equation of motion, we recover the retarded Green function using the prescription of Eq.(2.25).

Note that there is another prescription which was discovered before the one that we have discussed above; see [42], [43].

As shown in Appendix A, the spectral function, which measures the density of states, is $-1/\pi$ times the imaginary part of the retarded Green function. In a Fermi liquid with a sharply defined quasiparticle pole, the retarded Green function takes the following form near the Fermi surface:

$$G^R(\omega, k_\perp) = \frac{Z}{\omega - v_F k_\perp + i\gamma}. \tag{2.26}$$

Here ω is the energy of excitation, $k_\perp = k - k_F$ where k_F is the Fermi momentum, γ is the decay rate of the quasiparticle and Z is called the quasiparticle residue. Note that the above expression implies that G^R has a pole only in the lower half plane, consistent with the findings in Appendix A. We can now calculate the spectral function $A(\omega, k_\perp)$ from the imaginary part of this expression:

$$A(\omega, k_\perp) = \frac{1}{\pi} \frac{Z\gamma}{(\omega - v_F k_\perp)^2 + \gamma^2}. \tag{2.27}$$

In the limit of small γ, we see that this is equal to

$$A(\omega, k_\perp) = Z\delta(\omega - v_F k_\perp), \tag{2.28}$$

which is a delta-function peaked at the Fermi surface and zero frequency.

Chapter 3

Nonrelativistic Gauge/Gravity Duality

We know that the conformal group contains the Poincaré group as a subgroup. The Poincaré group is the group of spacetime symmetries of a relativistic field theory. To deal with the nonrelativistic field theories, we would like to consider a conformal extension of the Galilean group, which is the group of spacetime symmetries of a nonrelativistic system. The largest such extension is called the Schrödinger group since it is also the symmetry group of the free Schrödinger equation. See [44] for an introduction to nonrelativistic conformal field theories and the associated symmetry algebra.

A metric whose set of isometries coincides with the Schrödinger group was first constructed in [29] and [30]. The metric is called the vacuum Schrödinger metric and is given by

$$ds^2 = \frac{r^2}{R^2}\left(-r^2dt^2 + d\vec{x}^2 + 2d\xi dt\right) + \frac{R^2}{r^2}dr^2. \tag{3.1}$$

An important thing to notice is that scale transformations act differently on space and time. If $\vec{x}$ is scaled by a scale factor λ and r by $1/\lambda$, then time is scaled by λ^2 [1]. The peculiar thing is that there are *two* extra dimensions in the bulk, r and ξ. We

[1] It is possible to generalize the time scaling to λ^z, where the exponent z is called the *dynamical exponent*. We will always work with $z = 2$ in which case the coordinate ξ does not transform under scale transformations.

will see that this complicates our calculations significantly. In the symmetry algebra, there are two symmetry generators, the dilatation operator and the number operator, that may be simultaneously diagonalized and whose eigenvalues label inequivalent representations of the algebra. The role of the extra ξ direction is to geometrize the number operator $N = \partial_\xi$, just as the radial direction r geometrizes the dilatation operator $D = r\partial_r$.

As a brief digression, we make the following remark. If we omit the $d\xi dt$ term from the metric Eq.(3.1), we obtain a metric that describes Lifshitz fixed points. The symmetry group of this metric does not enjoy the full conformal invariance but only has translation, rotation and scale invariance. It is also possible to add black holes in this system. See [45] and [46]. In reference [47] this geometry was used to build a model for strange metals.

In subsequent work by various groups, blackhole horizons were added to Schrödinger spacetimes by starting with the black D3-brane solution of type IIB supergravity and transforming it using a technique from string theory called the null Melvin twist [33], [34], [35]. However, the extremal limit of these solutions was just the vacuum solution. Charged Schrödinger blackholes with proper extremal limits were constructed in [36], [37].

The metric of a charged Schrödinger blackhole, with a five-dimensional bulk and a three-dimensional boundary theory is given by

$$\frac{ds^2}{M^{1/3}} = \frac{Mr^2}{R^2}\left(-f d\tau^2 + dy^2 - \beta^2 r^2 f(d\tau + dy)^2\right) + \frac{r^2}{R^2}(dx_1^2 + dx_2^2) + \frac{R^2}{r^2}\frac{dr^2}{f}. \quad (3.2)$$

Here τ, y, x_1, x_2 and r are the bulk coordinates. It will be useful for us to work in slightly different coordinates: t, ξ, x_1, x_2, r, where

$$t = \beta(\tau + y), \quad \xi = \frac{1}{2\beta}(-\tau + y). \quad (3.3)$$

The metric in these coordinates is given by

$$M^{1/3} \times ds^2 = \frac{Mr^2}{R^2}\left(\left(\frac{1-f}{4\beta^2} - r^2 f\right)dt^2 + \beta^2(1-f)d\xi^2 + (1+f)dtd\xi\right) + \frac{r^2}{R^2}(dx_1^2 + dx_2^2) + \frac{R^2}{r^2}\frac{dr^2}{f} \tag{3.4}$$

It is the t coordinate that is identified with the time coordinate of the boundary theory. The τ coordinate is the relevant time coordinate near the horizon since it is the isometry direction that is null on the blackhole horizon, and thus determines the temperature. The boundary theory has the coordinates t, x_1, x_2. The functions f and M are given by

$$f(r) = 1 + \frac{Q^2}{r^6} - \left(r_0^4 + \frac{Q^2}{r_0^2}\right)\frac{1}{r^4}, \tag{3.5}$$

$$M(r) = \frac{1}{1 + \beta^2 r^2(1 - f(r))}. \tag{3.6}$$

Note that $f(r)$ is the same as the one in Eq.(2.12) with $n = 4$. The function f vanishes at r_0 and so, r_0 is the location of the horizon. Q is the charge of the black hole. The vacuum metric of Eq.(3.1) can be recovered by first taking $Q = 0$ and the taking $r_0 = 0$, in which case $f(r) = M(r) = 1$ for all r.

The gauge field A is purely in the τ direction and is given by

$$A = A_\tau \mathbf{d}\tau, \quad A_\tau = \frac{Q}{R^2 r_0^2}\left(1 - \frac{r_0^2}{r^2}\right), \tag{3.7}$$

which is obtained from Eq.(2.14) with $n = 4$ and a suitable choice of g_F. The temperature of the blackhole can be calculated by calculating the surface gravity starting from the Killing vector field

$$\frac{1}{\beta}\partial_\tau = \partial_t - \frac{1}{2\beta^2}\partial_\xi. \tag{3.8}$$

We have divided the generator ∂_τ by β to get the correct normalization of the boundary time coordinate t. Doing the calculation, one finds that the temperature is given

by

$$T = \frac{r_0}{\pi\beta R^2}\left(1 - \frac{Q^2}{2r_0^6}\right), \tag{3.9}$$

which is equal to $1/\beta$ times the expression in Eq.(2.13) with $n = 4$. The zero temperature case thus corresponds to $Q = \sqrt{2}r_0^3$.

The quantity β is a physical parameter that enters into the expression for various thermodynamic quantities of the boundary theory. Looking at Eq.(3.8), we see that from a thermodynamic point of view, we are working in the grand canonical ensemble with the chemical potential given by

$$\mu_1 = -\frac{1}{2\beta^2}. \tag{3.10}$$

This is the chemical potential that is associated with the invariant particle number in the field theory that is represented by the ξ-momentum in the bulk theory. There is another chemical potential that is associated with the global $U(1)$ current dual to the gauge field. The value of that chemical potential is given by

$$\mu_2 = \lim_{r\to\infty} A_t = \frac{Q}{2\beta R^2 r_0^2}. \tag{3.11}$$

We will consider a probe fermion field in an extremal (zero temperature) charged Schrödinger blackhole in a five-dimensional spacetime, and compute the spectral function of the dual operator in the three-dimensional nonrelativisitic CFT using the holographic duality.

Chapter 4

Setup of the Calculation

4.1 Dirac Equation in Curved Spacetimes

The Dirac equation for a spinor ψ carrying a charge q under the Maxwell field A_μ in a curved spacetime background is given by:

$$e_{\hat{a}}{}^{\mu}\Gamma^{\hat{a}}\mathcal{D}_\mu\psi = m\psi, \tag{4.1}$$

where m is the mass of the spinor, $\Gamma^{\hat{a}}$ are the Gamma matrices, $e_{\hat{a}}{}^{\mu}$ are a set of orthonormal vectors forming a basis for the tangent space of the spacetime manifold and $\mathcal{D}_\mu$ is the covariant derivative operator. The Gamma matrices satisfy the following anticommutation relations:

$$\{\Gamma^{\hat{a}}, \Gamma^{\hat{b}}\} = 2\eta^{\hat{a}\hat{b}}, \tag{4.2}$$

where η is the signature of the metric tensor $g_{\mu\nu}$. The $e_{\hat{a}}{}^{\mu}$ are called *vielbeins* and being an orthonormal basis, they satisfy the following identity:

$$g_{\mu\nu}e_{\hat{a}}{}^{\mu}e_{\hat{b}}{}^{\nu} = \eta_{\hat{a}\hat{b}}. \tag{4.3}$$

The covariant derivative $\mathcal{D}_\mu$ is given by:

$$\mathcal{D}_\mu = \partial_\mu + \frac{1}{8}\omega_{\hat{a}\hat{b}\mu}[\Gamma^{\hat{a}}, \Gamma^{\hat{b}}] - iqA_\mu, \tag{4.4}$$

where $\omega_{\hat{a}\hat{b}\mu}$ is a quantity called the *spin connection* and can be expressed in terms of the vielbeins and the metric tensor as follows:

$$\omega_{\hat{a}\hat{b}\mu} = e_{\hat{a}\nu}\partial_\mu e_{\hat{b}}{}^{\nu} + \Gamma^{\nu}{}_{\sigma\mu} e_{\hat{a}\nu} e_{\hat{b}}{}^{\sigma}, \tag{4.5}$$

where $\Gamma^{\nu}{}_{\sigma\mu}$ are the Christoffel symbols

$$\Gamma^{\nu}{}_{\sigma\mu} = \frac{1}{2} g^{\nu\lambda} \left(\partial_\sigma g_{\mu\lambda} + \partial_\mu g_{\sigma\lambda} - \partial_\lambda g_{\sigma\mu} \right). \tag{4.6}$$

4.2 Dirac Equation for Our System

We deal with a $(2+1)$-dimensional field theory, which corresponds to a 5-dimensional bulk theory. The bulk coordinates are labelled t, ξ, x_1, x_2, r and are always referred to in that order. We set both the curvature radius R and the location of the blackhole horizon r_0 equal to 1. The boundary is at $r = \infty$. We deal only with the extremal case (the case of zero temperature) in which the charge of the black-hole is $Q = \sqrt{2}$.

4.2.1 Vielbeins

We choose the following matrix as our vielbeins. The elements of a row constitute the contravariant components of one of the vectors. Thus the row index is a and the column index is μ.

$$e_{\hat{a}}{}^{\mu} = M^{\frac{1}{6}} \begin{bmatrix} \frac{\beta^2(f-1)}{2r^2 f B} & \frac{f+1+2\sqrt{f/M}}{4r^2 f B} & 0 & 0 & 0 \\ B & \frac{B(f+1-2\sqrt{f/M})}{2\beta^2(f-1)} & 0 & 0 & 0 \\ 0 & 0 & 1/r & 0 & 0 \\ 0 & 0 & 0 & 1/r & 0 \\ 0 & 0 & 0 & 0 & r\sqrt{f} \end{bmatrix}. \tag{4.7}$$

Here B is a function of r chosen in such a way that $\omega_{\hat{t}\hat{\xi}\hat{r}} = 0$. This also ensures that the coefficient of $\Gamma^{\hat{t}}\Gamma^{\hat{\xi}}\Gamma^{\hat{r}}$ in the Dirac equation is zero. Up to an overall multiplicative

constant, B is determined by the following equation

$$\frac{B'}{B} = -\frac{9r^6 + r^4 - 8r^2 + 4}{r(r^2-1)(r^2+2)(3r^2-2)} + \frac{6r^4}{3r^2-2}\sqrt{\frac{1}{(r^2+2)(r^4+3\beta^2r^2-2\beta^2)}}.$$

This equation implies that the boundary behavior of B is a constant times $1/r$. We choose that constant to be 1. This equation also implies that the near-horizon behavior of B is a constant times $1/(r-1)$, and we denote that constant by B_h. We can numerically solve this equation to find B_h. We get $B_h = 0.2222679212\ldots$ for $\beta = 1/\sqrt{2}$. An analytic expansion of B in the UV for $\beta = 1/\sqrt{2}$ is given by

$$B(r \to \infty) \simeq \frac{1}{r} + \frac{3}{4r^3} + \frac{15}{16r^5} + \frac{187}{256r^7} + \cdots$$

4.2.2 Gamma Matrices

We use 4×4 Gamma matrices, which are expressed in 2×2 blocks as follows:

$$\Gamma_\tau = \begin{bmatrix} 0 & i\sigma_3 \\ i\sigma_3 & 0 \end{bmatrix}, \quad \Gamma_y = \begin{bmatrix} 0 & -iI \\ iI & 0 \end{bmatrix}$$

$$\Gamma_0 = \beta(\Gamma_\tau + \Gamma_y), \quad \Gamma_1 = \frac{-\Gamma_\tau + \Gamma_y}{2\beta}$$

$$\Gamma_2 = \begin{bmatrix} 0 & \sigma_2 \\ \sigma_2 & 0 \end{bmatrix}, \quad \Gamma_3 = \begin{bmatrix} 0 & \sigma_1 \\ \sigma_1 & 0 \end{bmatrix}, \quad \Gamma_4 = \begin{bmatrix} I & 0 \\ 0 & I \end{bmatrix}$$

4.2.3 Explicit Form of the Dirac Equation

The spinor-field ψ has mass m and charge q. Next, we define ϕ_+ and ϕ_- by writing the spinor ψ as

$$\psi = (-gg^{rr})^{-1/4} \begin{pmatrix} \phi_+ \\ \phi_- \end{pmatrix} e^{-i\omega t + iL\xi + ik_1x_1 + ik_2x_2}. \tag{4.8}$$

After doing the calculations, we can write the Dirac equation as follows:

$$\boxed{\left(r\sqrt{f}\partial_r \mp mM^{-1/6}\right)\phi_\pm \pm \left(\pm u + v\sigma_3 + i\frac{k_1}{r}\sigma_2 + i\frac{k_2}{r}\sigma_1\right)\phi_\mp = 0}, \tag{4.9}$$

where u and v are simple linear combinations of the vielbein components $e_{\hat{t}}{}^{t}$,$e_{\hat{t}}{}^{\xi}$, $e_{\hat{\xi}}{}^{t}$ and $e_{\hat{\xi}}{}^{\xi}$:

$$u = \left[(\omega + qA_t)\left(-\beta e_{\hat{t}}^{\,t} - \frac{1}{2\beta}e_{\hat{\xi}}^{\,t}\right) + (L - qA_\xi)\left(\beta e_{\hat{t}}^{\,\xi} + \frac{1}{2\beta}e_{\hat{\xi}}^{\,\xi}\right)\right] M^{-\frac{1}{6}}, \tag{4.10}$$

$$v = \left[(\omega + qA_t)\left(\beta e_{\hat{t}}^{\,t} - \frac{1}{2\beta}e_{\hat{\xi}}^{\,t}\right) + (L - qA_\xi)\left(-\beta e_{\hat{t}}^{\,\xi} + \frac{1}{2\beta}e_{\hat{\xi}}^{\,\xi}\right)\right] M^{-\frac{1}{6}}. \tag{4.11}$$

By symmetry, we will always work with the case $k_1 = 0$. We set $k_2 = k$ from here on. We also write $\phi_+ = (y_+\ z_+)^{\mathrm{T}}$ and $\phi_- = (y_-\ z_-)^{\mathrm{T}}$ in component form.

4.3 UV Behavior ($r \to \infty$)

We use the Frobenius method to seek power series solutions of Eq.(4.9). Keeping two leading terms in the series, we can write the solution as:

$$\begin{aligned}
\phi_+(r) = {} & c\, r^{\nu_+ - \frac{1}{2}}(A_1 + A_2 r^{-2}) \\
& + \gamma\, r^{-\nu_+ - \frac{1}{2}}(\alpha_1 + \alpha_2 r^{-2}) \\
& + b\, r^{\nu_- + \frac{1}{2}}(B_1 + B_2 r^{-2}) \\
& + \beta\, r^{-\nu_- + \frac{1}{2}}(\beta_1 + \beta_2 r^{-2}),
\end{aligned}
\qquad
\begin{aligned}
\phi_-(r) = {} & c\, r^{\nu_+ + \frac{1}{2}}(C_1 + C_2 r^{-2}) \\
& + \gamma\, r^{-\nu_+ + \frac{1}{2}}(\gamma_1 + \gamma_2 r^{-2}) \\
& + b\, r^{\nu_- - \frac{1}{2}}(D_1 + D_2 r^{-2}) \\
& + \beta\, r^{-\nu_- - \frac{1}{2}}(\delta_1 + \delta_2 r^{-2}).
\end{aligned} \tag{4.12}$$

Here $\nu_\pm$ are given by

$$\nu_\pm = \sqrt{(L + qQ\beta)^2 + \left(m \pm \frac{1}{2}\right)^2}\,.$$

We see that there are four independent Frobenius-type solutions, which we have multiplied by the complex-valued constants c, γ, b and β. The spinors C_1, C_2, γ_1 and γ_2 are in the null space of $1 + \sigma_3$. Analogously, the spinors B_1, B_2, β_1 and β_2 are in

the null space of $1 - \sigma_3$. The normalization conventions are as follows:

$$C_{1-} = \alpha_{1-} = B_{1+} = \delta_{1+} = 1,$$

where the $+$ and $-$ subscripts denote the upper and lower components of the 2-spinors, respectively. All other components of the 2-spinors appearing the above expansion are fixed by this normalization and the UV behavior. We computed them analytically using Mathematica.

4.4 Evolution of the Retarded Green Function

The numbers c and b above are identified as sources, and γ and β as the corresponding responses. We treat the above expansion as exact; we can do so provided we regard c, γ, b and β, and hence also the Green function matrix G, as functions of r. Using Eq.(4.9), we obtain evolution equations for $c(r), \gamma(r), b(r)$ and $\beta(r)$, and finally for the 2×2 matrix $G(r)$. Thus, when the smoke clears, we have four non-linear, coupled, complex-valued first-order equations. By construction, the components of $G(r)$ must approach constants as $r \to \infty$. The task is to study the behavior of the eigenvalues of the asymptotic value of $G(r)$ as functions of L, ω and k.

Using the near-horizon ($r \to 1$) behavior, we calculate the infalling boundary conditions (which is necessary to obtain the retarded Green function) which we use as the initial data for the equations for $G(r)$. We do this in the next section.

Let us now derive for the evolution equations for $G(r)$. For a given set of c, γ, b and β, we define the column vectors,

$$S = [c \quad b]^{\mathrm{T}} \quad \text{and} \qquad R = [\gamma \quad \beta]^{\mathrm{T}}.$$

Then, we get two linearly independent solutions and define the 2×2 matrices S and R by setting their columns equal to the two linearly independent solutions. Then,

the Green function is given by

$$R = GS, \quad G = RS^{-1}. \tag{4.13}$$

Define the matrices "conv" and "Der" by

$$[c\ \gamma\ b\ \beta]^{\mathrm{T}} = \mathrm{conv}^{-1}\,[y_+\ z_+\ y_-\ z_-]^{\mathrm{T}}\,, \tag{4.14}$$

$$\left([y_+\ z_+\ y_-\ z_-]^{\mathrm{T}}\right)' = \mathrm{Der}\,[y_+\ z_+\ y_-\ z_-]^{\mathrm{T}}\,. \tag{4.15}$$

The matrix "conv" is obtained directly from Eq.(4.12) and the matrix "Der" is obtained directly from Eq.(4.9). Differentiate Eq.(4.14) to get

$$\begin{aligned}\left([c\ \gamma\ b\ \beta]^{\mathrm{T}}\right)' &= (\mathrm{conv}^{-1}\cdot\mathrm{Der}\cdot\mathrm{conv} - \mathrm{conv}^{-1}\cdot\mathrm{conv}')\,[c\ \gamma\ b\ \beta]^{\mathrm{T}} \\ &\equiv \mathrm{DER}\,[c\ \gamma\ b\ \beta]^{\mathrm{T}}\,.\end{aligned} \tag{4.16}$$

Taking the relevant subparts of DER gives 2×2 matrices A, B, C, D such that the equations for for R and S are

$$S' = AS + BR, \quad R' = CS + DR. \tag{4.17}$$

Differentiating the second part of Eq.(4.13), which is the defining equation for G, and using Eq.(4.17), we get

$$\boxed{G' = C + DG - G(A + BG)}. \tag{4.18}$$

4.5 In-falling Boundary Condition

We put $r = 1 + \epsilon$, and consider the small ϵ expansion of the equations. For later purposes, we will find it useful to define the quantities

$$\tilde{\omega} = \frac{L}{2\beta} + \beta\omega, \quad \alpha = \frac{\tilde{\omega}}{12}. \tag{4.19}$$

$\tilde{\omega}$ is the coefficient of τ in the exponential dependence of Eq.(4.8) when written in terms of the τ and y coordinates. We find that the behavior of x,y and f in the IR is given by

$$\begin{aligned} x &\to \frac{-12B_h^2+\beta^4}{24\beta^2 B_h\epsilon}\left(\frac{L}{2\beta}+\beta\omega\right) \equiv \frac{i2\sqrt{3}\alpha X}{\epsilon}, \\ y &\to \frac{-12B_h^2-\beta^4}{24\beta^2 B_h\epsilon}\left(\frac{L}{2\beta}+\beta\omega\right) \equiv \frac{i2\sqrt{3}\alpha Y}{\epsilon}, \\ f &\to 12\epsilon^2. \end{aligned}$$

Above, we have defined the quantities X and Y, which are explicitly written below:

$$X = \frac{i}{2}\left(\frac{2\sqrt{3}B_h}{\beta^2} - \frac{\beta^2}{2\sqrt{3}B_h}\right), \quad Y = \frac{i}{2}\left(\frac{2\sqrt{3}B_h}{\beta^2} + \frac{\beta^2}{2\sqrt{3}B_h}\right). \tag{4.20}$$

The Dirac equation near the horizon then becomes

$$\epsilon^2\phi'_\pm = -i\alpha(X \pm Y\sigma_3)\phi_\mp.$$

We make the ansatz $\phi_\pm \propto e^{i\tilde{\alpha}/\epsilon}$, where $\tilde{\alpha}$ is yet to be determined. Putting this back in the two equations, combining them and using the fact that $\tilde{\alpha}$ must be of the same sign as $\tilde{\omega}$ in order to satisfy the in-falling condition with respect to the coordinate τ, we get that $\tilde{\alpha} = \alpha$. Now when we put this pack into one of the two equations, we discover the in-falling boundary condition

$$\boxed{\phi_+|_H = (X + Y\sigma_3)\phi_-|_H}, \tag{4.21}$$

where the subscript H stands to remind us that the functions are evaluated at the horizon. Note that this is valid only for $\tilde{\omega} \neq 0$.

Explicitly this means that the two linearly independent choices are:

$$\begin{aligned} [s_{1+}\ r_{1+}\ s_{1-}\ r_{1-}]^{\mathrm{T}} &= \mathrm{conv}^{-1} \times \begin{bmatrix} X+Y & 0 & 1 & 0 \end{bmatrix}^{\mathrm{T}}, \\ [s_{2+}\ r_{2+}\ s_{2-}\ r_{2-}]^{\mathrm{T}} &= \mathrm{conv}^{-1} \times \begin{bmatrix} 0 & X-Y & 0 & 1 \end{bmatrix}^{\mathrm{T}}. \end{aligned}$$

We now form the initial S, R and G matrices as follows:

$$S|_H = \begin{bmatrix} s_{1+} & s_{2+} \\ s_{1-} & s_{2-} \end{bmatrix}, \quad R|_H = \begin{bmatrix} r_{1+} & r_{2+} \\ r_{1-} & r_{2-} \end{bmatrix}$$

$$\boxed{G|_H = R|_H \times S^{-1}|_H}. \tag{4.22}$$

The problem now is to study the differential equation Eq.(4.18) with the boundary condition Eq.(4.22).

Chapter 5

Results

Throughout this chapter we set $q = 1$ and $m = 0.1$ for the purpose of numerical computations. For convenience we define the gauge-invariant ξ-momentum:

$$\tilde{L} = L + qQ\beta.$$

5.1 Fermi Surfaces

We calculated the Green function for various values of the ξ-momentum L, the frequency ω and the spatial momentum k. The ξ momentum adds an extra parameter to our system and thus significantly complicates matters as compared to the relativistic case considered in [15], [16]. The ξ-momentum is related to the conserved particle number in nonrelativistic CFTs.

A typical plot of the spectral function is shown in Figure 5-1. This plot is for $L+qQ\beta = 0.1$ and $\beta = 1/\sqrt{2}$. The x-axis is the spatial momentum k and the different curves correspond to different values of ω. The curve with the the peak at the leftmost corresponds to $\omega = 0.9$ and the successive curves correspond to $\omega = 0.8, 0.7, \ldots, 0.1$. Note that the height of the peak for the $\omega = 0.9$ curve is supposed to be higher; the top is cut off because the sampling of the k values is not fine enough. We can confirm this by looking at the real part.

At a critical value of ω, called ω_F the profile of the imaginary part becomes

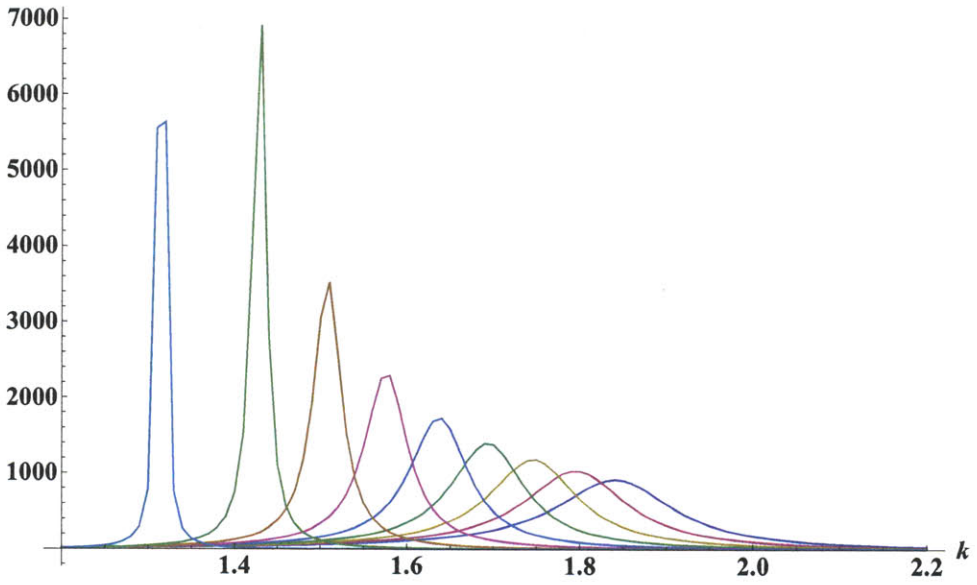

Figure 5-1: Plots of the spectral function for $\beta = 1/\sqrt{2}$ and $L + qQ\beta = 0.1$, i.e. $L = -0.9$. The x-axis represents the spatial momentum k. There are nine different plots in this figure, each for a different value of the frequency ω, in increments of 0.1. The rightmost plot is for $\omega = 0.1$ and the leftmost plot is for $\omega = 0.9$. The leftmost peak is clipped due to coarseness of the sampled k values. The peak develops into a delta-function at a particular value k_F of k and ω_F of ω. These values depend on the value of L.

a delta function located at a special value of k called the *Fermi momentum* and denoted by k_F. This is the signature of a Fermi surface. For this particular value of L, $k_F = 1.219$, $\omega_F \simeq 0.9$, which are determined numerically by tracking the peak locations for different values of ω.

The ω versus k relation near the Fermi surface is an important characteristic of a physical system. This is generically given by a power law of the form

$$\omega - \omega_F = A(k - k_F)^z. \tag{5.1}$$

Here the quantities of interest are ω_F, k_F and z, which all functions of L. For $L + qQ\beta = 0.1$, we have $z = 1.63$. This is consistent with a general argument due to Senthil [48] which shows that $z > 1$.

Thus, we have found a holographic description of Fermi surfaces in our system, extending the relativistic case considered in [15] [16]. This is important since there

are many condensed matter systems that have the Schrödinger symmetries.

The real part of the retarded Green function also has a distinctive feature at k_F. Figure 5-2 and Figure 5-3 show the real part of the eigenvalue for the same value of $L+qQ\beta = 0.1$. For values of ω away from ω_F the curve has the shape of a bump. The centers of the bumps correspond to the peaks in the curves of the imaginary parts. The bump develops a discontinuity at ω_F and k_F, which defines the Fermi surface. Note that the height of the bump increases a lot as we approach the Fermi surface.

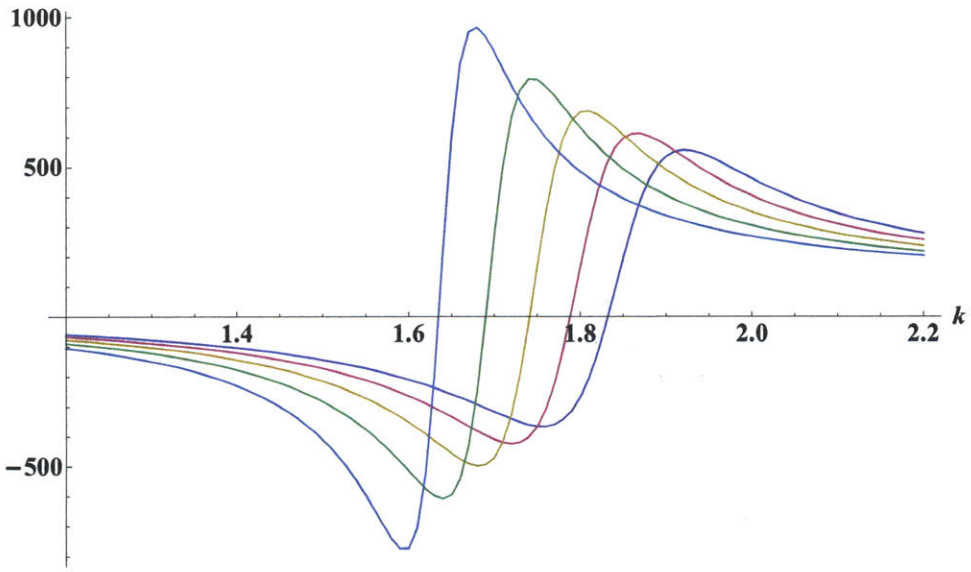

Figure 5-2: Plots of real part of the first eigenvalue of the Green function for $\beta = 1/\sqrt{2}$ and $L + qQ\beta = 0.1$. The x-axis represents the spatial momentum k. There are five different plots in this figure, each for a different value of the frequency ω, in increments of 0.1. The rightmost plot is for $\omega = 0.1$ and the leftmost plot is for $\omega = 0.5$. The hump develops into a discontinuity at special values k_F of k and ω_F of ω: see Figure 5-3. These values depend on the value of L.

We have found that for different values of L, the value of ω_F is given simply by

$$\omega_F = -\frac{L}{2\beta^2} = \mu_1 L. \tag{5.2}$$

This corresponds to zero $\tilde{\omega}$: the frequency for the τ coordinate defined in Eq.(4.19). The quantity μ_1 is the chemical potential associated with the ξ direction and is defined in Eq.(3.10). This is physically meaningful since the τ coordinate is the appropriate

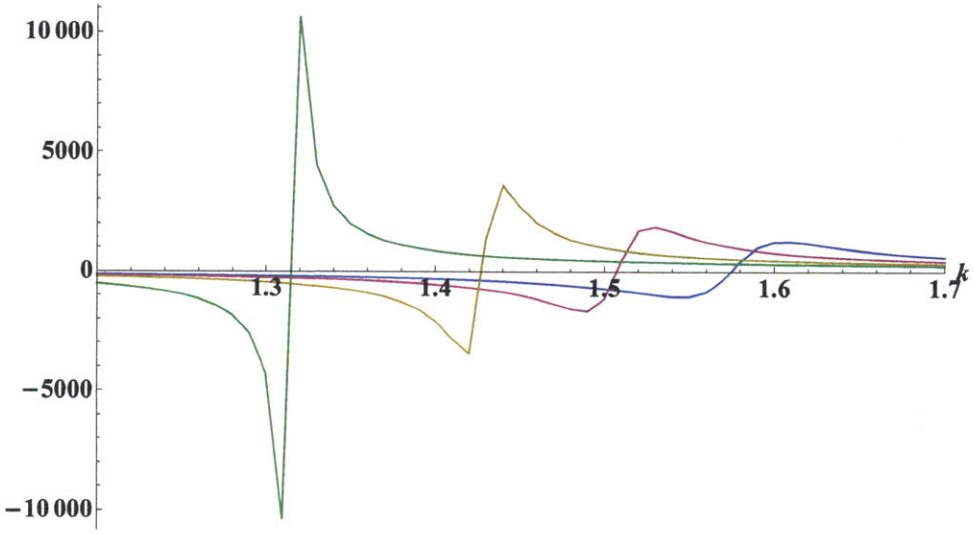

Figure 5-3: Plots of real part of the first eigenvalue of the Green function for $\beta = 1/\sqrt{2}$ and $L + qQ\beta = 0.1$. There are four different plots in this figure; the rightmost plot is for $\omega = 0.6$ and the leftmost plot is for $\omega = 0.9$ in increments of 0.1. Looking at the numbers on the y-axis reveals that the humps are much higher than in Figure 5-2. The hump develops into a discontinuity at special values k_F of k and ω_F of ω. These values depend on the value of L.

time coordinate near the horizon and the low-frequency excitations are governed by by the IR geometry. In particular, fermionic systems have gapless excitations about the Fermi surface and usually $\omega_F = 0$. The quantity ω is the frequency conjugate to the t coordinate which is the appropriate time coordinate for the boundary theory. The Fermi surface is offset by an amount equal to the chemical potential due L: the ξ-momentum (recall that the ξ momentum is related to the conserved particle number in nonrelativistic systems).

Table 5.1 collects the values of k_f and z obtained numerically for various values of $\tilde{L}$. Note that the k_f decreases and z increases with increasing $\tilde{L}$.

$\tilde{L}$	k_f	z
0.05	2.31	1.37
0.10	1.22	1.63
0.20	0.40	1.80

Table 5.1: Table of values of the fermi momentum k and the scaling exponent z for various values of the ξ momentum $L = \tilde{L} - qQ\beta$. In this table, $\beta = 1/\sqrt{2}$.

5.2 Near-Horizon AdS_2 Scaling

The near-horizon geometry of the metric in Eq.(3.4) is $AdS_2 \times \mathbb{R}^3$; see [37], [36]. As was shown in [16] for the relativistic case, this fact enables us to analytically calculate the low-frequency behavior of the spectral function. We look for power-law solutions for ϕ_+ and ϕ_- in the $r \to 1$ region, and find that they behave like $r^{\pm\nu}$, where

$$\nu = \sqrt{k^2 + \frac{4m^2}{9} + \mu}\,, \tag{5.3}$$

with the quantity μ being given by:

$$\mu = \frac{1}{18}\left(49 + \frac{21}{\sqrt{2}} - \frac{\left(42 + 115\sqrt{2}\right)(L+1)}{\sqrt{2}} + \left(54 + \frac{21}{\sqrt{2}}\right)(L+1)^2\right), \tag{5.4}$$

where we have set $q = 1$ and $\beta = 1/\sqrt{2}$.

5.3 Vanishing of Fermi Surfaces

As shown in [16], when the quantity ν defined in Eq.(5.3) is imaginary for $k = k_F$, there is no Fermi surface. In the specific numerical case $m = 0.1, q = 1$ and $\beta = 1/\sqrt{2}$,

$$\nu = \sqrt{k^2 + 3.825(\tilde{L} - 1.470)(\tilde{L} - 0.632)}, \tag{5.5}$$

and thus, ν cannot be imaginary at $\tilde{L} = 0.1$ consistent with the existence of a Fermi surface. However, if for the same values m, q, β, we pick $\tilde{L} = 1$, we get $\nu = \sqrt{k^2 - 0.662}$, and this will be imaginary if the value of the Fermi momentum is greater than 0.814. Indeed $k_F > 0.814$, as illustrated by the trends in Table 5.1.

Chapter 6

Summary and Conclusions

In this thesis, we have reviewed and provided elementary exposition of the various theoretical tools needed for AdS/CFT. A discussion of AdS spaces, blackhole solutions, the AdS/CFT correspondence, Green functions and the nonrelativistic gauge/gravity duality has been given.

We have created a setup to solve for the retarded Green functions in a three-dimensional nonrelativistic boundary field theory at finite density and zero temperature. This setup has been discussed in detail in this thesis.

Our numerical calculations have confirmed the existence of holographic Fermi surfaces in the nonrelativistic gauge/gravity duality. This shows that the Fermi surfaces found earlier in the relativistic setting are robust.

We also calculated the near-horizon scaling exponent, a critical quantity that controls the low-energy physics. We exhibited the dependence of this exponent on the momentum along the extra direction in the bulk. We showed that just by tuning this momentum, the exponent can be made imaginary.

Appendix A

Formal Properties of Green Functions

In this appendix, we state the defintions and some relations between the various Green functions and the spectral function. The main result that we are looking for is contained in Eq.(A.13) which states that the spectral function is simply related to the imaginary part of the retarded (or advanced) Green function. We mainly follow the exposition given in Chapter 3 of [49].

This result is interesting because the starting definitions of the retarded Green function and the spectral function are different. The retarded Green function describes the linear response of an operator induced by a small perturbation in the Hamiltonian. The spectral function describes the density of states and has delta-function poles at the allowed excitation energies.

First, a brief point about notation. We define the fourier transform of a function $f(t)$ as

$$f(E) = \int_{-\infty}^{\infty} dt\, e^{iEt} f(t). \tag{A.1}$$

Note that we use the same letter for a function and its fourier transform.

Consider two bosonic operators A and B in the Heisenberg picture. We first obtain convenient expressions for the two correlation functions: $\langle A(t)B(t')\rangle$ and $\langle B(t')A(t)\rangle$, where the average is taken over the canonical ensemble if the temperature is nonzero.

At zero temperature the average just means the matrix element of the operators in the ground state, since we expect that zero temperature the system will be in its ground state. Let $\zeta = \mathrm{Tr}\left(e^{-\beta H}\right)$ be the partition function, with $\beta = 1/T$ and H the Hamiltonian of the system. We can also average over the grand canonical ensemble provided we use the grand canonical Hamiltonian $\mathcal{H} = H - \mu N$, but we choose to work in the canonical ensemble. We make the following manipulations:

$$\begin{aligned}
\zeta\langle A(t)B(t')\rangle &= \mathrm{Tr}\left(e^{-\beta H}A(t)B(t')\right) \\
&= \sum_{m,n}\langle m|e^{-\beta H}A(t)|n\rangle\langle n|B(t')|m\rangle \\
&= \sum_{m,n} e^{-\beta E_m}\langle m|e^{iHt}Ae^{-iHt}|n\rangle\langle n|e^{iHt'}Be^{-iHt'}|m\rangle \\
&= \sum_{m,n} e^{-\beta E_m}e^{-i(E_n-E_m)(t-t')}\langle m|A|n\rangle\langle n|B|m\rangle
\end{aligned} \tag{A.2}$$

Next we expand $\langle B(t')A(t)\rangle$, which we can just get from the above formula by swapping A with B and t with t'. Thus, we get

$$\begin{aligned}
\zeta\langle B(t')A(t)\rangle &= \sum_{m,n} e^{-\beta E_m}e^{+i(E_n-E_m)(t-t')}\langle m|B|n\rangle\langle n|A|m\rangle \\
&= \sum_{m,n} e^{-\beta E_n}e^{-i(E_n-E_m)(t-t')}\langle m|A|n\rangle\langle n|B|m\rangle,
\end{aligned} \tag{A.3}$$

where in the last step we interchanged the dummy variables m and n. This is convenient since now the only difference between Eq.(A.2) and Eq.(A.3) is the Boltzmann weight. Eq.(A.2) and Eq.(A.3) are very useful and will be repeatedly used in the analysis below.

The *spectral function* $S_{AB}(t,t')$ is defined as

$$S_{AB}(t,t') \equiv \frac{1}{2\pi}\langle[A(t),B(t')]\rangle. \tag{A.4}$$

If A and B are fermionic operators, we use the anticommutator instead of the commutator in the above definition. Time translation invariance implies that the spectral

function depends only on the difference $t-t'$. Using the above two expressions for the correlation functions, it is straightforward to get an expression for the spectral functions and fourier transform it. The only t dependence is in the imaginary exponential and we get a delta function.

$$\boxed{S_{AB}(E) = \frac{1}{\zeta}\sum_{m,n}\left(e^{-\beta E_m} - e^{-\beta E_n}\right)\delta(E-(E_n-E_m))\langle m|A|n\rangle\langle n|B|m\rangle}. \quad \text{(A.5)}$$

We can easily understand the various components of this formula. The real exponentials are the Boltzmann weights of the energy eigenstates, the delta function is the density of states, and the matrix elements give transition "probabilities" induced by the operators A and B. Typically A and B are chosen to be hermitian conjugates, and then the product of matrix elements that appears above actually becomes the probability.

The *retarded Green function* and the *advanced Green function* are defined as

$$G^{\text{ret}}_{AB}(t,t') \equiv -i\theta(t-t')\langle[A(t),B(t')]\rangle, \quad \text{(A.6)}$$

$$G^{\text{adv}}_{AB}(t,t') \equiv +i\theta(t'-t)\langle[A(t),B(t')]\rangle. \quad \text{(A.7)}$$

Again, for fermionic operators, the commutator is replaced by the anticommutator.

It can be shown that if we perturb the Hamiltonian by the term $f(t)B$ where f is a c-number function, then the change in the expectation value of A is given by

$$\delta\langle A(t)\rangle = \int_{-\infty}^{\infty} dt' G^{\text{ret}}_{AB}(t,t')f(t').$$

Here the time-dependence of the operators is in the interaction picture.

Let us take the definition of the retarded Green function and replace the products of operators by the expression found above for the correlation functions. Next, we fourier transform this to get:

$$G^{\text{ret}}_{AB}(E) = \frac{-i}{\zeta}\sum_{m,n}\left(e^{-\beta E_m} - e^{-\beta E_n}\right)\langle m|A|n\rangle\langle n|B|m\rangle\int_0^{\infty} dt e^{-i(E_n-E_m)t}e^{iEt}. \quad \text{(A.8)}$$

Now the integral will yield $i/(E-(E_n-E_m))$, but we have to add a small positive imaginary part to E to make the integral converge at plus infinity. Exploiting the delta function that appears in Eq.(A.5), we can write

$$\boxed{G^{\text{ret}}_{AB}(E) = \int_{-\infty}^{+\infty} d\xi \frac{S_{AB}(\xi)}{E-\xi+i\epsilon}}. \tag{A.9}$$

The calculation for the advanced Green function is exactly similar except that we need to make the integral convergent at minus infinity, so we have to add a small negative imaginary part to E.

$$\boxed{G^{\text{adv}}_{AB}(E) = \int_{-\infty}^{+\infty} d\xi \frac{S_{AB}(\xi)}{E-\xi-i\epsilon}}. \tag{A.10}$$

The expressions Eq.(A.9) and Eq.(A.10) imply that we can extend the retarded Green function analytically in the upper half of the complex E plane and the advanced Green function in the lower.

Next, we use Eq.(A.9) and Eq.(A.10) to get the spectral function in terms of the retarded and advanced Green functions. Using the fact that

$$\lim_{\epsilon\to 0} \frac{\epsilon}{x^2+\epsilon^2} = \pi\delta(x), \tag{A.11}$$

it is straightforward to get

$$S_{AB}(E) = \frac{i}{2\pi}\left(G^{\text{ret}}_{AB}(E) - G^{\text{adv}}_{AB}(E)\right). \tag{A.12}$$

Further if we assume that the spectral function is purely real, then Eq.(A.9) and Eq.(A.10) imply that the retarded and the advanced Green functions are complex conjugates and this we get

$$\boxed{S_{AB}(E) = -\frac{1}{\pi}\text{Im}\left(G^{\text{ret}}_{AB}(E)\right) = \frac{1}{\pi}\text{Im}\left(G^{\text{adv}}_{AB}(E)\right)}. \tag{A.13}$$

The assumption of reality of the spectral function holds for most practical choices of

A and B. Eq.(A.13) is the main result that we were seeking: the spectral function, whose pole structure gives the location of the excitation energies, is simply related to the imaginary part of the retarded Green function, which is a linear response function.

Bibliography

[1] Juan Martin Maldacena, "The large N limit of superconformal field theories and supergravity," Adv. Theor. Math. Phys. **2**, 231–252 (1998), arXiv:hep-th/9711200

[2] S. S. Gubser, Igor R. Klebanov, and Alexander M. Polyakov, "Gauge theory correlators from non-critical string theory," Phys. Lett. **B428**, 105–114 (1998), arXiv:hep-th/9802109

[3] Edward Witten, "Anti-de Sitter space and holography," Adv. Theor. Math. Phys. **2**, 253–291 (1998), arXiv:hep-th/9802150

[4] Gary T. Horowitz and Juan Martin Maldacena, "The black hole final state," JHEP **02**, 008 (2004), arXiv:hep-th/0310281

[5] Juan Martin Maldacena, "D-branes and near extremal black holes at low energies," Phys. Rev. **D55**, 7645–7650 (1997), arXiv:hep-th/9611125

[6] Raphael Bousso, "The holographic principle," Rev. Mod. Phys. **74**, 825–874 (2002), arXiv:hep-th/0203101

[7] Ofer Aharony, Steven S. Gubser, Juan Martin Maldacena, Hirosi Ooguri, and Yaron Oz, "Large N field theories, string theory and gravity," Phys. Rept. **323**, 183–386 (2000), arXiv:hep-th/9905111

[8] Sean A. Hartnoll, "Lectures on holographic methods for condensed matter physics," Class. Quant. Grav. **26**, 224002 (2009), arXiv:0903.3246 [hep-th]

[9] Christopher P. Herzog, "Lectures on Holographic Superfluidity and Superconductivity," J. Phys. **A42**, 343001 (2009), arXiv:0904.1975 [hep-th]

[10] S. Sachdev and M. Müller, "Quantum criticality and black holes," Journal of Physics Condensed Matter **21**, 164216 (Apr. 2009), arXiv:0810.3005 [cond-mat]

[11] John McGreevy, "Holographic duality with a view toward many-body physics," (2009), arXiv:0909.0518 [hep-th]

[12] Steven S. Gubser, "Breaking an Abelian gauge symmetry near a black hole horizon," Phys. Rev. **D78**, 065034 (2008), arXiv:0801.2977 [hep-th]

[13] Sean A. Hartnoll, Christopher P. Herzog, and Gary T. Horowitz, "Building a Holographic Superconductor," Phys. Rev. Lett. **101**, 031601 (2008), arXiv:0803.3295 [hep-th]

[14] Sean A. Hartnoll, Christopher P. Herzog, and Gary T. Horowitz, "Holographic Superconductors," JHEP **12**, 015 (2008), arXiv:0810.1563 [hep-th]

[15] Hong Liu, John McGreevy, and David Vegh, "Non-Fermi liquids from holography," (2009), arXiv:0903.2477 [hep-th]

[16] Thomas Faulkner, Hong Liu, John McGreevy, and David Vegh, "Emergent quantum criticality, Fermi surfaces, and AdS2," (2009), arXiv:0907.2694 [hep-th]

[17] Thomas Faulkner, Nabil Iqbal, Hong Liu, John McGreevy, and David Vegh, "From black holes to strange metals," (2010), arXiv:1003.1728 [hep-th]

[18] Thomas Faulkner, Nabil Iqbal, Hong Liu, John McGreevy, and David Vegh, "Strange metal transport realized by gauge/gravity duality," Science **329**, 1043–1047 (2010)

[19] Subir Sachdev, "Holographic metals and the fractionalized Fermi liquid," Phys. Rev. Lett. **105**, 151602 (2010), arXiv:1006.3794 [hep-th]

[20] T. Senthil, Subir Sachdev, and Matthias Vojta, "Fractionalized Fermi Liquids," Phys. Rev. Lett. **90**, 216403 (2003)

[21] Subir Sachdev, "Strange metals and the AdS/CFT correspondence," Journal of Statistical Mechanics: Theory and Experiment **11**, 22 (2010), arXiv:1010.0682 [cond-mat.str-el]

[22] John McGreevy, "In pursuit of a nameless metal," Physics **3**, 83 (2010)

[23] Thomas Faulkner, Gary T. Horowitz, John McGreevy, Matthew M. Roberts, and David Vegh, "Photoemission 'experiments' on holographic superconductors," JHEP **03**, 121 (2010), arXiv:0911.3402 [hep-th]

[24] Sean A. Hartnoll and Pavel Kovtun, "Hall conductivity from dyonic black holes," Phys. Rev. **D76**, 066001 (2007), arXiv:0704.1160 [hep-th]

[25] Sean A. Hartnoll, Pavel K. Kovtun, Markus Müller, and Subir Sachdev, "Theory of the Nernst effect near quantum phase transitions in condensed matter and in dyonic black holes," Phys. Rev. **B76**, 144502 (2007), arXiv:0706.3215 [cond-mat.str-el]

[26] Sean A. Hartnoll and Christopher P. Herzog, "Ohm's Law at strong coupling: S duality and the cyclotron resonance," Phys. Rev. **D76**, 106012 (2007), arXiv:0706.3228 [hep-th]

[27] Sean A. Hartnoll and Christopher P. Herzog, "Impure AdS/CFT," Phys. Rev. **D77**, 106009 (2008), arXiv:0801.1693 [hep-th]

[28] Frederik Denef, Sean A. Hartnoll, and Subir Sachdev, "Quantum oscillations and black hole ringing," Phys. Rev. **D80**, 126016 (2009), arXiv:0908.1788 [hep-th]

[29] Koushik Balasubramanian and John McGreevy, "Gravity duals for non-relativistic CFTs," Phys. Rev. Lett. **101**, 061601 (2008), arXiv:0804.4053 [hep-th]

[30] Dam T. Son, "Toward an AdS/cold atoms correspondence: a geometric realization of the Schroedinger symmetry," Phys. Rev. **D78**, 046003 (2008), arXiv:0804.3972 [hep-th]

[31] Amin Akhavan, Mohsen Alishahiha, Ali Davody, and Ali Vahedi, "Fermions in non-relativistic AdS/CFT correspondence," Phys. Rev. **D79**, 086010 (2009), arXiv:0902.0276 [hep-th]

[32] Koushik Balasubramanian and John McGreevy, "The particle number in Galilean holography," (2010), arXiv:1007.2184 [hep-th]

[33] Allan Adams, Koushik Balasubramanian, and John McGreevy, "Hot Spacetimes for Cold Atoms," JHEP **11**, 059 (2008), arXiv:0807.1111 [hep-th]

[34] Christopher P. Herzog, Mukund Rangamani, and Simon F. Ross, "Heating up Galilean holography," JHEP **11**, 080 (2008), arXiv:0807.1099 [hep-th]

[35] Juan Maldacena, Dario Martelli, and Yuji Tachikawa, "Comments on string theory backgrounds with nonrelativistic conformal symmetry," JHEP **10**, 072 (2008), arXiv:0807.1100 [hep-th]

[36] Allan Adams, Charles Max Brown, Oliver DeWolfe, and Christopher Rosen, "Charged Schrodinger Black Holes," Phys. Rev. **D80**, 125018 (2009), arXiv:0907.1920 [hep-th]

[37] Emiliano Imeroni and Aninda Sinha, "Non-relativistic metrics with extremal limits," JHEP **09**, 096 (2009), arXiv:0907.1892 [hep-th]

[38] Barton Zwiebach, *A First Course in String Theory* (Cambridge University Press, 2009)

[39] Nabil Iqbal and Hong Liu, "Real-time response in AdS/CFT with application to spinors," Fortsch. Phys. **57**, 367–384 (2009), arXiv:0903.2596 [hep-th]

[40] Thomas Faulkner, Hong Liu, and Mukund Rangamani, "Integrating out geometry: Holographic Wilsonian RG and the membrane paradigm," (2010), arXiv:1010.4036 [hep-th]

[41] Nabil Iqbal and Hong Liu, "Universality of the hydrodynamic limit in AdS/CFT and the membrane paradigm," Phys. Rev. **D79**, 025023 (2009), arXiv:0809.3808 [hep-th]

[42] Dam T. Son and Andrei O. Starinets, "Minkowski-space correlators in AdS/CFT correspondence: Recipe and applications," JHEP **09**, 042 (2002), arXiv:hep-th/0205051

[43] Christopher P. Herzog and Dam T. Son, "Schwinger-Keldysh propagators from AdS/CFT correspondence," JHEP **03**, 046 (2003), arXiv:hep-th/0212072

[44] Yusuke Nishida and Dam T. Son, "Nonrelativistic conformal field theories," Phys. Rev. **D76**, 086004 (2007), arXiv:0706.3746 [hep-th]

[45] Shamit Kachru, Xiao Liu, and Michael Mulligan, "Gravity Duals of Lifshitz-like Fixed Points," Phys. Rev. **D78**, 106005 (2008), arXiv:0808.1725 [hep-th]

[46] Koushik Balasubramanian and John McGreevy, "An analytic Lifshitz black hole," Phys. Rev. **D80**, 104039 (2009), arXiv:0909.0263 [hep-th]

[47] Sean A. Hartnoll, Joseph Polchinski, Eva Silverstein, and David Tong, "Towards strange metallic holography," JHEP **04**, 120 (2010), arXiv:0912.1061 [hep-th]

[48] T. Senthil, "Critical fermi surfaces and non-fermi liquid metals," Phys. Rev. **B78**, 035103 (2008), arXiv:0803.4009 [cond-mat]

[49] Wofgang Nolting, *Fundamentals of Many-body Physics* (Springer, 2009)